Experimental and Computational Studies of Welding Parameters on Weld Performance in Friction Stir Welded Materials- Review

K. Samadhanam Raju[1*], N. Ramanaiah[2]
[1]Research Scholar, Mechanical Engineering, AU College of Engineering (A), Visakhapatnam, 530003, India.
[2]Professor, Mechanical Engineering, AU College of Engineering (A), Visakhapatnam, 530003, India.
*Corresponding Author: samadhanamrajukaranam@gmail.com

Article Info
Page Number: 89- 102
Publication Issue:
Vol 71 No. 4 (2022)

Abstract

Friction Stir Welding (FSW) is an exceptional technique used to join various materials which maybe either similar or dissimilar. It is a simple solid state welding procedure which uses a rotating tool for generating the heat by friction and join the metal parts. In this paper, a review was conducted on the effects of various welding parameters like welding speed, rotational speed of tool, force applied on the interface of the rotating tool shoulder and the work piece, pin profile of the tool, tilting angle of the tool etc. on mechanical properties and microstructural development of different materials joined by FSW method. In addition, the temperature distribution and material flow using different analytical softwares also described. FSW can be extensively used in aviation, marine and vehicle body construction manufacturing because of its good mechanical properties.

Article History
Article Received*: 25 March 2022*
Revised*: 30 April 2022*
Accepted*: 15 June 2022*
Publication*: 19 August 2022*

Keywords: - Friction stir welding (FSW); Dissimilar friction stir welding (DFSW); Welding parameters; Microstructure; Mechanical properties.

Introduction:

The Welding Institute (TWI) developed and patented FSW solid state welding method in the year 1991 (Thomas et al., 1991), in which the welding is processed below the work piece' melting point. During FSW, there is no external heat given to the work piece, but produced within the materials to be joined by friction between the work material and the rotating tool. This process has several benefits over the conventional (fusion) welding process like low residual stresses, low distortion and high strength of the weld joint. This process (Figure 1) is carried out in three stages mainly according to the relative motion between rotating tool and metallic work piece in a given time period. In the first stage, known as plunge period, the rotating tool is plunged vertically into the weld line and after that dwell period follows, the second stage, in which the tool keeps on rotating at that particular position without moving towards the other end along the weld line. In the third stage, due to friction, heat is produced and dissipated to the adjacent material and leads to an increase of temperature. Welding process parameters considered mostly are: the welding speed, rotational speed of tool, force applied on the interface of tool shoulder and work piece, shape of the tool pin, tilting angle of tool etc. The microstructure development of aluminum friction stir welds is categorized into four different regions such as unaffected or parent zone, heat affected zone-HAZ, thermo-mechanically affected zone-TMAZ and nugget or stirred zone-SZ.

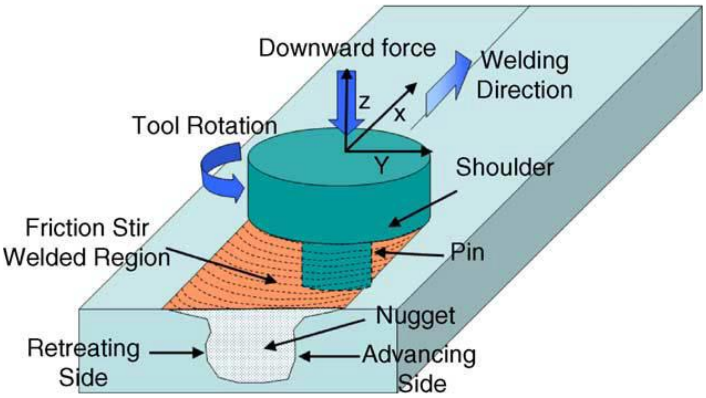

Figure 1. FSW process

Influence of various welding parameters on mechanical properties of various materials joined by FSW:

Table 1 shows the influence of several welding considerations on mechanical properties of dissimilar friction stir welds (DFSW). The welding parameters considered: tool rotational speed in rpm, welding speed in mm/min, force applied on the interface of tool shoulder and work piece in kN, profile of the tool pin, tilting angle of the tool in deg. etc. and these were optimized by different researchers for various DFSW. In the current paper, the mechanical properties such as ultimate tensile strength (UTS) in N/mm^2, yield strength (YS) in N/mm^2, percentage of elongation in %, joint efficiency in percentage in %, hardness of the base materials and different DFSWs were presented.

S.No.	Name of the Author	Base Metal/Tool material	Mechanical properties	Welding parameters
1	Lan Zhang et al., 2020	BM: 6061 T6 Al Alloy	Max.UTS=233MPa, YS=155MPa, HV=92, δ=5%	1500rpm, 450mm/min
2	Gihad Karrar et al., 2020	BM: AA5083 & Commercially pure Copper Tool: High strength steel tool	Max. UTS=203MPa, Joint efficiency=94.8%	1400rpm, 120mm/min
3	Anton Noumav et al., 2020	BM: Al-Cu-Li Alloy	Max.UTS=376MPa, δ=3.8%	800rpm, 200mm/min
4	Y. Tao et al., 2020	BM: 2060 T8 Al-Li Alloy	Max.UTS=444.8MPa, δ=12.5%	1200rpm, 200mm/min
5	Junping Li et al., 2020	BM: Ti-6Al-4V alloy Tool: W-Re alloy pin and	Max.UTS=1062.2MPa, YS=980.5MPa, δ=14.1%, HV=337.4	1000rpm, 30mm/min

		Ni based super alloy shoulder		
6	S. Shashi Kumar et al., 2020	BM: AISI 316L SS Tool: Tungsten Lanthanum Oxide	Max.UTS=605MPa, YS=380MPa, Joint Efficiency= 96%	600rpm, 45mm/min, Axial load=11kN, Tilt angle=1.5^o
7	Taher A. Shehabeldeen et al., 2021	BM: Ti-6Al-4V & 6061 T6 Al Alloy Tool: Tungsten Carbide	Shear strength=3.5kN/mm^2, HV=384	1000rpm, 25mm/min
8	Xiaomeng Qin et al., 2020	BM: CoCrFeNi high entropy alloy Tool: WC	Max.UTS=627MPa, YS=476MPa, HV=245.7, δ=42%	200rpm, 50mm/min, Load=1500kg
9	Velaphi Msomi et al., 2020	BM: AA1050 H14 & AA6082 T6 Tool: HSS	Max.UTS=48MPa, YS=29MPa, δ=20.1%	1200rpm, 40mm/min, Tilt angle=2^o
10	M Zhou et al., 2019	BM: Duplex LZ91 Mg-Li Alloy Tool: Steel tool SKD61, WC Cemented Carbide tool	Max.UTS=151.2MPa, YS=129MPa, δ=33.4%	300rpm, 100mm/min
11	Edip Cetkin et al., 2019	BM: AA7075 & AA5182 Al Alloys Tool: K100 Steel	Max.UTS=265MPa, HV=87	980rpm, 108mm/min
12	Hongduo Wang et al., 2019	BM: SS304 & Q235 low carbon steel Tool: WC-Co stirring tool	Max.UTS=493MPa, δ=17%	475rpm, 47.5mm/min
13	Sree Sabari et al., 2016	BM: AA2519 T87 Al Alloy Tool: HSS	Max.UTS=282MPa, δ=10.4%, Joint Efficiency=62%	1100rpm, 30mm/min, Tilt angle=2^o
14	Huaibo Deng et al., 2020	BM: Ni50.7 Ti49.3 Alloy Tool: W-25 Re	Max.UTS=751MPa	600rpm, 60mm/min
15	Jianing Li et al., 2020	BM: 7A04 T6 Al Alloy	Max.UTS=452MPa, δ=4.24%	1000rpm, 120mm/min

ISSN: 2094-0343
2326-9865

16	Junlei Zhang et al., 2020	BM: AZ31 & AM60 Mg Alloys	Max.UTS=252MPa, YS=116MPa, δ=12.5%	1600rpm, 100mm/s

Table 1. Influence of various process parameters on mechanical properties of dissimilar friction stir welds (DFSW)

Microstructural study of various materials joined by the method FSW:

Figure.2 (a-c): shows the microstructures of the nugget or stir zone indicated as SZ, thermomechanically affected zone indicated as TMAZ & heat affected zone indicated as HAZ of FSW AA 7A04-T6. Jianing Li et al., 2020 carried out the experimentation on bonding of AA 7A04-T6 by FSW. They observed the microstructures of the sample 1 with rotational speed of 800rpm, welding speed of 120mm/min, sample 2 with rotational speed of 1000rpm, welding speed of 120mm/min and sample 3 with rotational speed of 1200rpm, welding speed of 120mm/min by using Scanning Electron Microscope (SEM). They concluded that the sample 2 gives the optimum results.

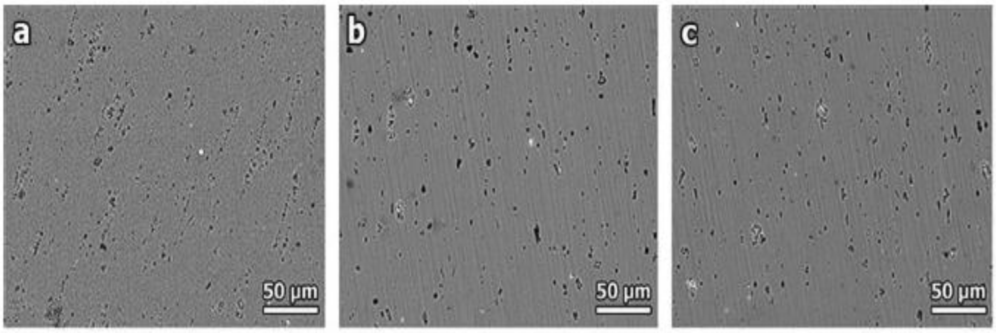

Figure 2. Microstructures of sample 2 (a) SZ, (b) TMAZ, (c) HAZ

They also done the refinement of the microstructure behavior, firming the mechanical properties of this FSW joint by laser local heat treatment (LLHT) method. Figure 3 shows the microstructure of total cross section of FSW of AA 6061-T6. Lan Z et al., 2020 explored the microstructural, mechanical properties & behavior of the growth of the crack of AA 6061-T6 by FSW at rotational speed of 1500rpm & welding speed of 450mm/min. They observed that the size of grain, hardness and the impact absorbing energy of the weld nugget or stir zone indicated as WNZ lesser than the parent material zone and heat affected region.

Figure 3. Microstructure of overall cross section

It was found that "S" defects shown in above figure were observed in the stir zone, the weak joint flaw occurs regularly in aluminum alloy joined by FSW. The weak joint flaw was maybe formed due to the oxide on butt surface of the work pieces with the application of shear of head that was stirring because of more welding speed, less amount of input heat and the oxide layer was broken inadequacy.

Gihad Karrar et al., 2020 explored the microstructural characterization & mechanical properties of DFSW AA5083-Cu. They observed that the transversion of AA5083 (aluminum side) to Cu DFSW welded at tool rotational speed of 1000rpm & welding speed of 100mm/min. Relatively minor Cu particles found as often circulated between Al interface region & upper surface of the nugget or stir region towards the Al side. And at the weld nugget region, larger Cu particles strained and unevenly distributed along nugget or stir region in the direction of bottom of the interfacial area between nugget region & Cu side. The uneven Cu elements formed a lamella configuration of copper and aluminum at the lower end of the thermo mechanically affected zone towards the Cu side. Figure 4 shows the zones formed in the weld joint cutaway section in DFSW of AA7075/AA5182. Edip Cetkin et al., 2019 examined microstructural, mechanical properties of AA7075/AA5182 joined by FSW. Microstructures of welding joints were inspected in their study by an optical microscope and SEM. And the configurations containing of base metal or parent zone as BM, heat affected zone as HAZ, thermomechanically affected zone as TMAZ and stir zone or dynamic recrystallization zone as DCZ zones examined in large & small size.

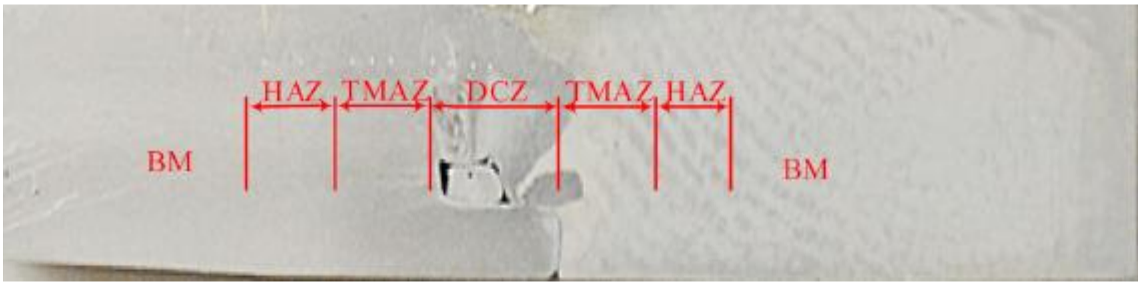

Figure 4. Zones in weld cutaway

They performed the experimentation with the two different tool pin profiles: conical and triangular shaped profiles. Figure 5 (a) represents microstructure of Al-Cu-Li alloy by optical microscopy, (b to e) represents the microstructure of the Al-Cu-Li alloy using TEM micrographs. Anton Noumav et al., 2020 studied the microstructural evolution and mechanical performance of Al-Cu-Li alloy welded by FSW. The transmission electron microscopy study was performed for the parent metal and various regions of weld joint to define precipitates and disruptions, density and dispersals.

ISSN: 2094-0343
2326-9865

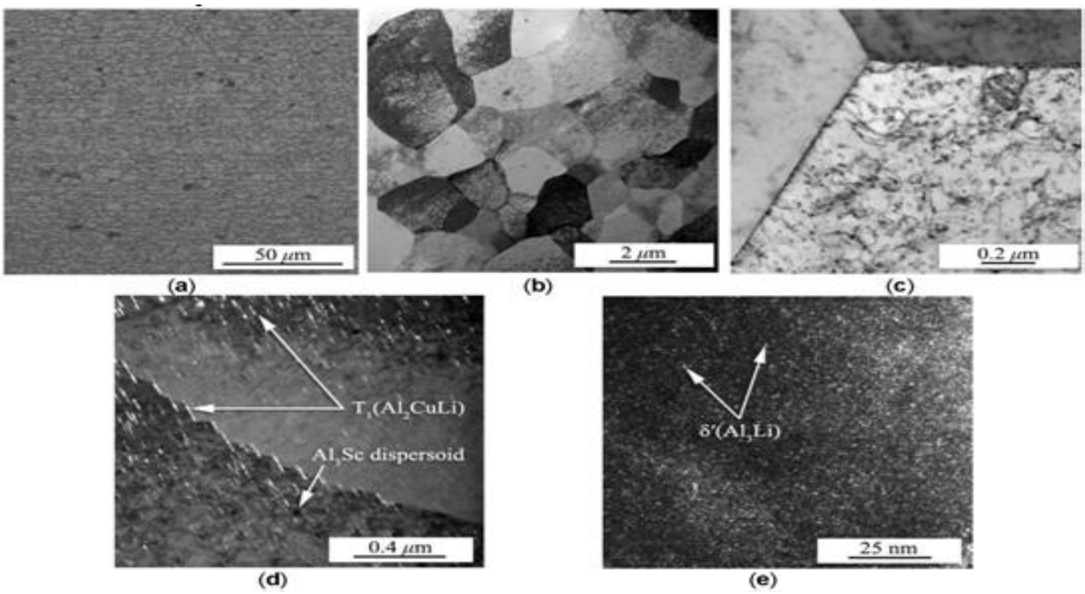

Figure 5. Microstructural behavior of parent material

optical microscopy (a) and TEM micrographs (b to e)

Figure 6 shows the visualization of the surface and SEM figures of cross-sections formed at traverse speed 25mm/min in DFSW of AA6061 T6 and Ti6Al4V. Taher A. Shehabeldeen et al., 2021 explored the microstructural, mechanical properties and also fracture mechanisms of DFSW AA6061 T6 and Ti6Al4V.

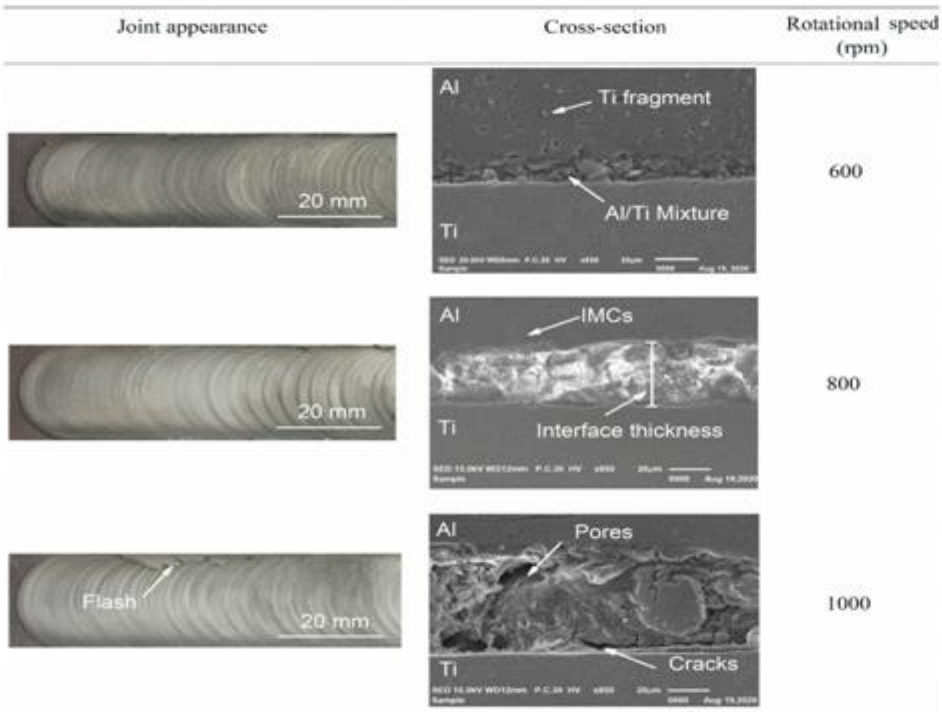

Figure 6. Surface look and SEM figures

They concluded that the interfacial microstructure varies considerably using various rotational speeds of the tool. An enough input heat causing generating a flaw free weld joint with a minor thickness of Aluminum/Titanium interface for the rotational speed of 600 rpm, while TiAl and $TiAl_3$ were the key phases formed at the interface, Ti fragments were evenly distributed alongside of aluminum. Super plastic deformation of Al/Ti mixture was occurred on increasing the rotational speed further up to 1000 rpm and that increases thickness of interface layer of Al/Ti results in brittle segments of inter metallic compounds that worsen the weld joint configuration. Figure 7 shows the microstructure of LZ91 base metal. Mengran Zhou et al., 2019 studied the microstructural & mechanical properties of duplex Mg–Li alloy LZ91 joined by FSW. The microstructures in nugget zone exhibited the refined grains and comprising of an Mg-rich α phase & a Li-rich β phase which are having approximately equal dimensions in all the directions. The grains in Mg-rich α phase exhibited uncertain crystal placements after the formation of dynamic recrystallization. They concluded that grain improvement and uniform mixing of Mg-rich α phase and Li-rich β phase attained in nugget zone after process. The grain measurement was increased with tool rotating speed.

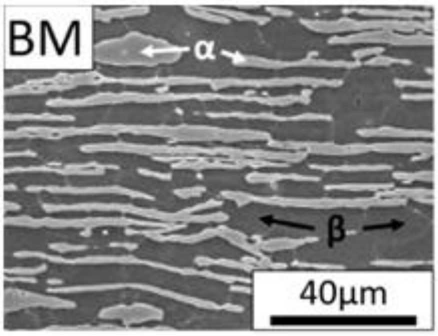

Figure 7. Microstructure of LZ91 base metal

Huaibo Deng et al., 2020 studied the microstructural, mechanical properties and also transformation performance of FSW Ni50.7 Ti49.3 alloy. The results indicated that IMCs were worsened the mechanical properties of weld joints and it was failed in advance the martensitic stage appeared. $W_{13}Re_7$ & Ti_2Ni coarse fashioned were dispersed at the tool shoulder affected zone, and that zone was castled.

Simulation study of various materials joined by FSW:

Figure 8 shows the comparison of the results obtained by the analytical solution, numerical solution using ABAQUS explicit software and experimentation in the transverse direction (at x=0.12m), and also the temperature contour of the Al-Cu FSW plates by ABAQUS. Solaleh Salimi et al., 2014 performed a 3 dimensional temperature field analysis considering the transient condition. They considered a moving heat source in circular shape as a welding beam and solved the heat conduction transient problem of dissimilar plates Al-Cu butted together. Four number of thermocouples were used for measuring the temperature within the translational region. They simulated this problem by a commercial FEM software ABAQUS and also established the temperature contour at the end of the welding procedure. And they compared the results.

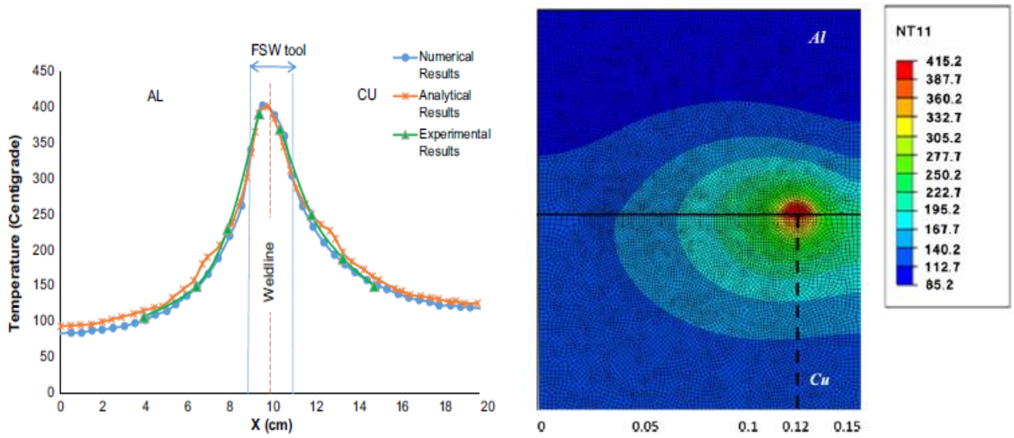

(a) (b)

Figure 8. a) Comparison of results b) Temperature contour by ABAQUS

Ling Long et al., 2017 developed a finite element analysis of tilting angle of tool, and its effect on development of friction stir joints. DEFORM-3D software was used to examine process, and the code Lagrangian implicit selected as numerical framework. And the results showed that wormhole flaws appear in weld of tilting angle 0° and no such type of defects were detected for the case of 2° tilting angle. The material flow in tail side of tool with tilting angle was enhanced considerably and that results in avoiding the wormhole defect occurrence on advancing side. Z. Zhang et al., 2009 investigated the influence of transverse speed on FSW & it was examined in detail for monitoring this parameter. They used a fully coupled and thermo-mechanical method for the analysis. ABAQUS/EXPLICIT software was used for the solution. They concluded that the FSW defect occurs for high welding speed. When the welding speed was greater, the performance of the rotating tool come to be weaker and this was the reason for weld defect. Figure 9 shows the temperature field of FSW 7075-T6 aluminum alloy at the final stage. S.D. Ji et al., 2013 explored the effect of temperature at different stages of FSW of Al 7075 T6 on the behavior of material transfer. The morphologies of weld of FSW Al 7075-T6 were examined by using optical microscopy, using ABAQUS software the temperature field was produced. The effect of temperature on behavior of material transfer in TMAZ at various stages examined. The relationships between temperature and the behavior of material transfer at various stages of welding were explored.

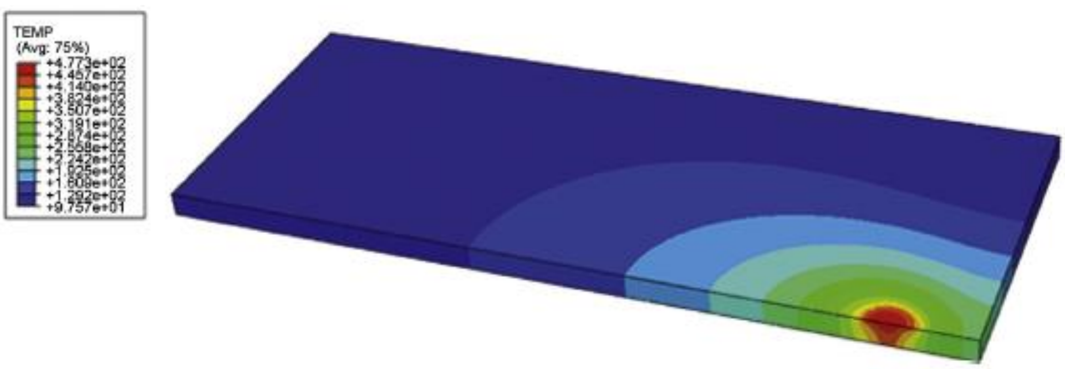

Figure 9. Temperature field at final stage

Figure 10 shows the distribution of temperature along crosswise of the similar AA2024 materials after 13s from starting of welding. Kun Li et al., 2017 used CEL (Coupled Eulerian Lagrangian) method to get the perfect modeling of similar AA2024 materials joined by FSW for the rotational speed of 800rpm and welding speed of 2mm/s. The materials were considered as Eulerian components and tool as Lagrangian. Johnson-Cook model used to model the behavior of the material of the plates during the process of simulation. They concluded that the distribution of temperature along the weld joint line was irregular with high temperature on advancing side and was greater than retreating side.

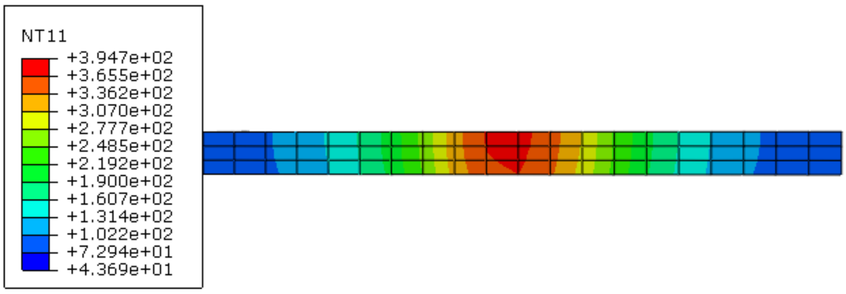

Figure 10. The distribution of temperature of the materials after 13s

Figure 11 shows the strain rate distribution during FSW Al-Cu-Li alloy for three different weld matrices. Anton Noumav et al., 2020 observed the microstructural development & mechanical performance of FSW Al-Cu-Li alloy. The transmission electron microscopy observation performed for the parent metal and various zones of welds to examine precipitates and disturbances, density and distributions. Thermo-Calc software was used for the assessment of TEM results. CFD modeling used to determine the distribution of temperature & strain rate during FSW for three various weld matrices: weld matrix 1 (100mm/min and 700rpm), weld matrix 2 (150mm/min and 700rpm) and weld matrix 3 (200mm/min and 800rpm) which gives the best results.

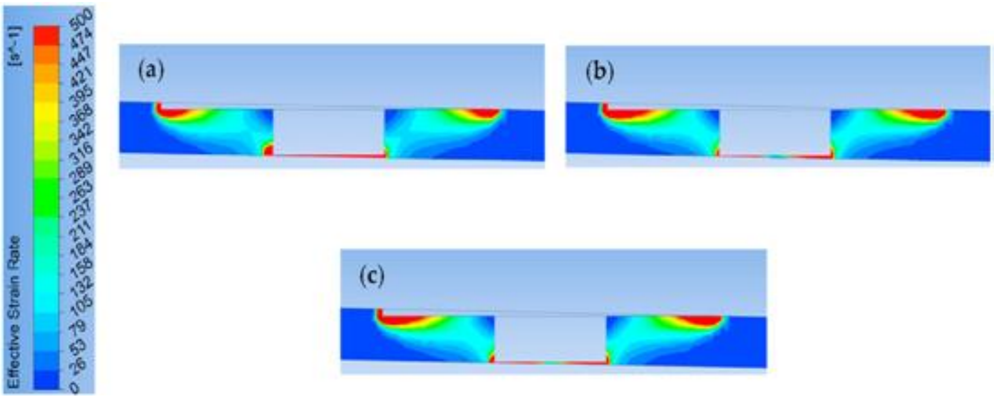

Figure 11. Strain rates

Figure 12 shows the surface temperature distribution during FSW of Al-Cu-Li alloy for three different weld matrices. The distribution of temperature in cross-section seems with isotherms due to the comparatively small thickness of the welded pieces, and are closely at right angles to the surface of the model.

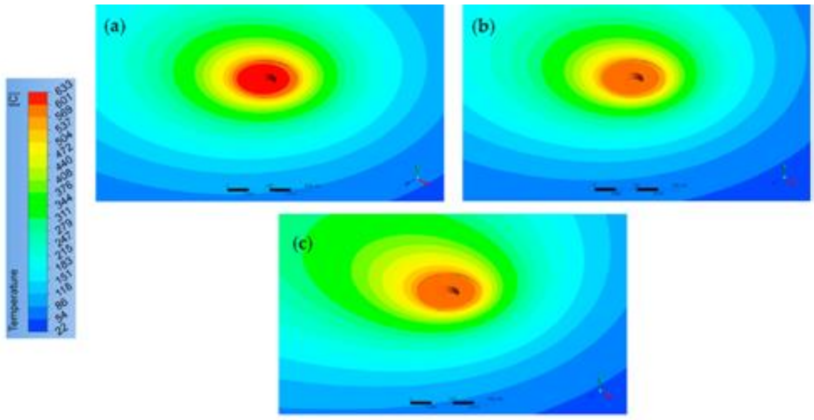

Figure 12. Temperature distribution

Figure 13 show the temperature field and material flow for 0º and 2.5º tool tilt angles in FSW of Aluminum alloy (AA6061-T6) plates. Ming Zhai et al., 2020 explored the effect of tilting angle of tool on heat transfer and the behavior of the material flow in FSW of Aluminum alloy (AA6061-T6) plates. They carried out the experiments at 0º and 2.5º tool tilting angle keeping the rotational speed 800rpm & welding speed 150mm/min constant. The measured peak temperatures were high at the interface of work piece and tool for the case of 2.5º tilting angle compared to 0º tilt angle. The CFD models (using Ansys Fluent) were established to examine the temperature distribution and material flow in FSW under various situations.

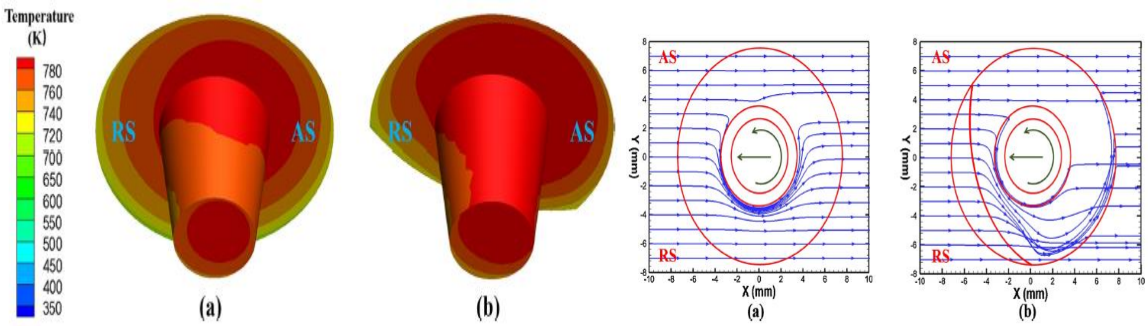

Figure 13. Temperature field and material flow for 0º (a) and 2.5º (b) tool tilt angles

Figure 14 shows the temperature distribution in work piece and tool during FSW. R. Keivani et al., 2013 explored the influence of tool pin angle & effect of preheating on the distribution of temperature during FSW process. A 3D model based on FEA was used to analyze thermal feature of Cu C11000 during the FSW process. The increase of tool pin angle improves the temperature about the weld joint line. But the preheating process does not disturb the distribution of the temperature along the weld joint line noticeably. Abaqus/Explicit software was used to model and analyze FSW process.

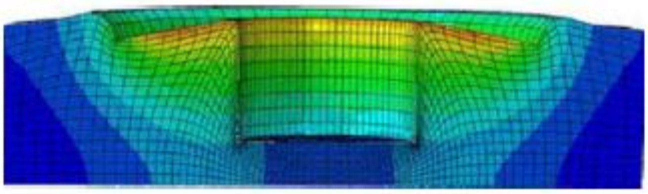

Figure 14. Temperature distribution in work piece and tool

Mir Zahedul H. Khandkar et al., 2006 expected the residual thermal stresses in FSW metals. They studied three dissimilar materials which are: AA-2024, AA-6061 & SS 304 L. ABAQUS software was used for the computational analysis. The performance of rotational tool was possibly accountable for relieving the stresses within the region of TMAZ to some extent that could otherwise be excessive due to heavy temperatures in that region and the firm holding of the weld parts. Vinayak Malik et al., 2014 explored the effect of several tool pin shapes in FSW using ABAQUS/Explicit considering CEL method. The process parameters considered are: tool rotational speed 950 rpm, plunging velocity10 mm/min, dwelling time10 s, welding speed 60 mm/min, plunging depth 0.2mm and tool tilting angle 0°. Six number of tool pin shapes of circular, triangular, square, rectangular, pentagonal and hexagonal pin were considered in their study. They concluded that square shape tool pin consumes low power among the remaining shapes without disturbing the generation of temperature. R. Padmanaban et al., 2014 carried out the simulation of the distribution temperature and the behavior of material flow during DFSW of AA2024 and AA7075 using CFD. The FSW process was modeled as a visco-plastic laminar stream past a rotational tool in steady state condition. They concluded that highest temperature in joined plates increases with the rise of tool rotating speed and the diameter of the shoulder, whereas the highest temperature decreases with the increase of welding speed. On increasing the tool rotational speed and diameter of the shoulder, the flow of material increases, while increasing the traverse speed reduces the flow of material in stir or nugget zone. GAMBIT software was used for meshing the model with 551470 hexahedral cells. J. Abhilash et al., 2018 simulated the FSW using thermo-mechanical coupled FEM analysis. ANSYS parametric design language was used for the simulation without using any filler metal. For geometry creation of FSW setup, SOLID 226 was used. The welding parameters considered in their model: diameter of tool, plunging depth, tool rotational speed & welding speed and which affects the highest temperature. H.W. Zhang et al., 2005 presented the 2D results of the flow of the material configurations and the residual stresses in FSW. A 2D model was established for FSW of an Al alloy using ABAQUS code. They concluded that material on advancing side of joint results in formation of a fluidized bed around tool pin but material on retreating side not ever revolves along with pin. The maximum longitudinal residual stress increased on increasing the velocity of translation of tool pin. H.W. Zhang et al., 2007 simulated the behavior of the flow of material in FSW considering various welding parameters using ABAQUS. In simulation, the loads applied axially on tool shoulder varies from 10 to 100MPa, welding speed applied to borders of welding plate varies from 2 to 10 mm/s, and rotational speeds of tool varies from 390 to 690 rpm. There exists a swirl on advancing side. On increasing the welding speed, the flow of material in swirl on advancing side to be quicker. Mahmoud Eskandari et al., 2019 studied the thermomechanical and micro structural issues in the welding zone in DFSW of AA6061 wrought and A390 cast compounds. A fully-coupled thermomechanical FEA code, ABAQUS/Explicit used for the solution. They concluded that the placement of materials either on advancing side or on retreating side. Livan Fratini et al., 2009 conducted simulation on a continuous finite element model in which FSW process was employed and predicted the residual stresses and fatigue life using the fatigue crack propagation using DEFORM-3D software. The work part modeled as a firm visco-plastic material, and rotational tool supposed to be rigid.

Conclusions:

From the above review, it could be concluded that, the input welding parameters like profile of the tool pin, tilting angle of tool, welding or traverse speed, rotational speed of tool, axial load etc. effect the mechanical properties & microstructures of friction stir welded materials which maybe either similar or dissimilar. And there is still a significant need to examine more different combinations of welding parameters even many studies have been performed. Numerical finite element simulation can be done by the use of various finite element analysis softwares like ABAQUS, ANSYS, DEFORM 3D etc. The simulation of effect of welding parameters on the distribution of temperature and residual stresses can be validated using the experimental results. And the results will be within a suitable range after validation. FSW can be adapted to various materials unlike fusion welding. It has wide variety of applications with its safe and echo friendly operation to the welders. It is a defect free joining process. And weld joint can be formed below the point of melting of base metal.

Conflict of Interest:

The authors have no conflict of interest to declare.

References:

[1] A. Abdollahzadeh et al., “The effect of changing chemical composition on dissimilar Mg/Al friction stir welded butt joints using zinc interlayer”, Journal of Manufacturing Processes, 2018, 34 18–30.

[2] Anton Noumav et al., “Microstructural evolution and mechanical performance of Al-Cu-Li alloy joined by friction stir welding”, Journal of materials research and technology, 2020, 9(6): 14454-14466.

[3] Anuj Bansal et al., “Influence of cryogenic treatment on mechanical performance of friction stir Al-Zn-Cu alloy weldments”, Journal of Manufacturing Processes, 2020, 56 43–53.

[4] Amlan Kar et al., “Effect of niobium interlayer in dissimilar friction stir welding of aluminum to titanium”, Materials Characterization, 2018, 145 402–412.

[5] Brandon A. McWilliams et al., “Numerical simulation and experimental characterization of friction stir welding on thick aluminum alloy AA2139-T8 plates”, Materials Science & Engineering A, 2013, 585 243–252.

[6] Edip Cetkin et. al., “Microstructure and mechanical properties of AA7075/AA5182 jointed by FSW”, Journal of Materials Processing Tech, 2019, 268 107–116.

[7] Gihad Karrar et al., “Microstructural characterization and mechanical properties of dissimilar AA5083-copper joints produced by friction stir welding”, j mater res technol, 2020, 9(5):11968–11979.

[8] Guolin Guo et al., “Interfacial properties of friction stir lap welded 430/304 stainless steels using Cu interlayer”, Materials Letters, 2021, 284 129027.

[9] Hongduo Wang et. al., “Microstructure and mechanical properties of dissimilar friction stir welded type 304 austenitic stainless steel to Q235 low carbon steel”, Materials Characterization, 2019, 155 109803.

[10] Huaibo Deng et. al., “Microstructure, mechanical properties and transformation behavior of friction stir welded Ni50.7Ti49.3 alloy”, Materials and Design, 2020, 189 108491.

[11] H.W. Zhang et al., “The finite element simulation of the friction stir welding process”, Materials Science and Engineering A, 2005, 403 340–348.

[12] H.W. Zhang et al., “3D modeling of material flow in friction stir welding under different process parameters”, Journal of Materials Processing Technology, 2007, 183 62–70.

[13] J. Abhilash et al., “Simulation of friction stir welding using thermo-mechanical coupled finite element method”, Materials Science and Engineering, 2018, 455 012113.

[14] Jianing Li et. al., “Mechanical property and characterization of 7A04-T6 aluminum alloys bonded by friction stir welding”, Journal of Manufacturing Processes, 2020, 52 263–269.

[15] Junlei Zhang et. al., “Optimizing the mechanical properties of friction stir welded dissimilar joint of AM60 and AZ31 alloys by controlling deformation behavior”, Materials Science & Engineering A, 2020, 773 138839.

[16] Junping Li et al., “Friction stir welding of Ti-6Al-4V alloy: Friction tool, microstructure and mechanical properties”, Journal of Manufacturing Processes, 2020, 58 344–354.
[17] K. Anderson Wedge et al., “Characterization of the evolution of 2219-T87 aluminum as a function of the friction stir welding process”, International Journal of Fatigue, 2021, 142 105954.
[18] Kun Li et al., “Using coupled Eulerian Lagrangian formulation for accurate modeling of the friction stir welding process”, Procedia Engineering, 2017, 207 574–579.
[19] Lan Zhang et al., “Microstructure, mechanical properties and fatigue crack growth behavior of friction stir welded joint of 6061-T6 aluminum alloy”, International Journal of Fatigue, 2020, 135 105556.
[20] Ling Long et al., “Finite-element analysis of the tool tilt angle effect on the formation of friction stir welds”, Journal of Manufacturing Processes, 2017, 30 562–569.
[21] Livan Fratini et al., “Residual stresses and FCP prediction in FSW through a continuous FE model”, Journal of Materials Processing Technology, 2009, 209 5465–5474.
[22] Mahmoud Eskandari et al., “The study of thermo mechanical and micro structural issues in dissimilar FSW of AA6061 wrought and A390 cast alloys”, Journal of Manufacturing Processes, 2019, 41 168–176.
[23] Mengran Zhou et. Al., “Microstructure and mechanical properties of friction stir welded duplex Mg–Li alloy LZ91”, Materials Science & Engineering A, 2019.
[24] Ming Zhai et al., “Influence of tool tilt angle on heat transfer and material flow in friction stir welding”, Journal of Manufacturing Processes, 2020, 59 98–112.
[25] Mir Zahedul et al., “Predicting residual thermal stresses in friction stir welded metals”, Journal of Materials Processing Technology, 2006, 174 195–203.
[26] Nikhil Gotawala et al., “Microstructural analysis and mechanical behavior of SS 304 and titanium joint from friction stir butt welding”, Materials Science & Engineering A, 2020, 789 139658.
[27] P. Murali Krishna et al., “Effect of post-weld heat treatment on the mechanical properties of friction stir welds of dissimilar aluminum alloys”, International Journal of Engineering Science and Technology, 2011, Vol. 3 No. 7, 5778-5785.
[28] P. Satish Kumar et al., “Effect of tool pin geometry on friction stir welded dissimilar aluminum alloys- (AA5083 and AA6061)”, International Journal of Mechanical Engineering and Technology, 2018, Volume 9, Issue 12, pp. 647-653.
[29] R. Keivani et al., “Effects of pin angle and preheating on temperature distribution during friction stir welding operation”, Trans. Nonferrous Met. Soc. China, 2013, 23 2708−2713.
[30] R. Padmanaban et al., “Numerical simulation of temperature distribution and material flow during friction stir welding of dissimilar aluminum alloys”, Procedia Engineering, 2014, 97 854 – 863.
[31] S.D. Ji et al., “Effect of temperature on material transfer behavior at different stages of friction stir welded 7075-T6 aluminum alloy”, J. Mater. Sci. Technol., 2013, 1-6
[32] Solaleh Salimi et al., “A 3D transient analytical solution to the temperature field during dissimilar welding processes”, International Journal of Mechanical Sciences, 2014, 79 66–74.
[33] Sree Sabari et. al., “Characteristics of FSW and UWFSW joints of AA2519-T87 aluminum alloy: Effect of tool rotation speed”, Journal of Manufacturing Processes, 2016, 22 278–289.
[34] S. Shashi Kumar et al., “Effect of tool tilt angle on weld joint properties of FSW AISI 316L stainless steel sheets”, Measurement, 2020, 150 107083.
[35] Thomas, W. M., Nicholas, E. D., Needam, J. C., Murch, M. G., Templesmith, P. and Dawes, C. J., GB Patent Application No. 9125978.8, December 1991 and US Patent No. 5460317, October 1995.
[36] Taher A. Shehabeldeen et.al., “Investigation of the microstructure, mechanical properties and fracture mechanisms of dissimilar friction stir welded aluminum/titanium joints”, Journal of Materials Research and Technology, 2021, 11, 507-518.
[37] Velaphi Msomi et. al., “Analysis of material positioning towards microstructure of the friction stir processed AA1050/AA6082 dissimilar joint”, Advances in Industrial and Manufacturing Engineering, 2020, 1 100002.
[38] V. Anand Kumar et al., “Effect of tool pin profile and friction stir welding speed on tensile & hardness properties of friction stir welded joints of AA6082 & A319 aluminium alloy”, International Journal of Innovative Technology and Exploring Engineering, 2019, Volume-8 Issue-12.

[39] Vinayak Malik et al., "Investigations on the effect of various tool pin profiles in friction stir welding using finite element simulations", Procedia Engineering, 2014, 97 1060 – 1068.

[40] V. Shokri et al., "Thermomechanical modeling of friction stir welding in a Cu-DSS dissimilar joint", Journal of Manufacturing Processes, 2018, 31 46–55.

[41] Wenshen Tang et al., "Numerical and experimental investigations on friction stir welding of Ti and Nb modified 12% Cr ferritic stainless steel", Journal of Manufacturing Processes, 2020, 59 223–237.

[42] Wentao Hou et al., "Enhancing metallurgical and mechanical properties of friction stir butt welded joints of Al–Cu via cold sprayed Ni interlayer", Materials Science & Engineering A, 2021, 809 140992.

[43] Wenyang Wang et al., "Microstructure and mechanical properties of dissimilar friction stir welds in austenitic-duplex stainless steels", Materials Science & Engineering A, 2020, 787 139499.

[44] Wen Wang et al., "Microstructure and nanomechanical behavior of friction stir welded joint of 7055 aluminum alloy", Journal of Manufacturing Processes, 2021, 61 311–321.

[45] Xiaomeng Qin et. al., "Effect of process parameters on microstructure and mechanical properties of friction stir welded CoCrFeNi high entropy alloy", Materials Science & Engineering A, 2020, 782 139277.

[46] Y. Tao et al., "Friction stir welding of 2060-T8 Al-Li alloy. Part I: Microstructure evolution mechanism and mechanical properties", Materials Characterization, 2020, 168 110524.

[47] Zexi Wu et al., "Microstructure and tensile properties of friction stir welded 0.2% C-Si-Mn steel", Materials Science & Engineering A, 2021, 799 140068.

[48] Z. Z. Xu et al., "Effect of base metal state on the microstructure and mechanical properties of Al-Mg-Si alloy friction stir welded joints", Journal of Manufacturing Processes, 2020, 56 248–257.

[49] Z. Zhang et al., "Numerical studies on the effect of transverse speed in friction stir welding", Materials and Design, 2009, 30 900–907.